Surfaces and Interfaces 21 (2020) 100760

Contents lists available at ScienceDirect

Surfaces and Interfaces

journal homepage: www.sciencedirect.com/journal/surfaces-and-interfaces

Corrosion performance of electrospinning nanofiber ZnO-NiO-CuO/polycaprolactone coated on mild steel in acid solution

Mothana Ghazi Kadhim AlFalah [a,b,*], Ersin Kamberli [d], Ali H. Abbar [c], Fatma Kandemirli [d], Murat Saracoglu [e]

[a] Metallurgy and Materials Engineering Department, Faculty of Engineering and Architecture, Kastamonu University, 37150, Kastamonu, Turkey
[b] Materials of Engineering Department, College of Engineering, University of Al–Qadisiyah, 58002, Al–Qadisiyah, Iraq
[c] Department of Biochemical Engineering, Al-Khwarizmi College of Engineering, University of Baghdad, Baghdad, Iraq
[d] Biomedical Engineering Department, Faculty of Engineering and Architecture, Kastamonu University, 37150, Kastamonu, Turkey
[e] Faculty of Education, Erciyes University, 38039, Kayseri, Turkey

A R T I C L E I N F O

Keywords:
Electrospinning
Mild steel
ZnO-NiO-CuO/PCL
Nanofiber
Corrosion resistance
EIS

A B S T R A C T

In the present work, PCL/ZnO (polycaprolactone/ zinc oxide), PCL/NiO (polycarprolactone/nickel oxide), PCL/CuO (polycarprolactone/copper oxide), and PCL/ZnO-NiO-CuO (polycarprolactone/ zinc oxide- nickel oxide-copper oxide) have been successfully fabricated and deposited on a mild steel through electrospinning technique. SEM, EDX, and FT-IR had been used to characterize all nanofiber coatings on the mild steel. A nanofiber layer of ZnO/NiO/CuO/PCL was utilized to coating the mild steel as a corrosion protector film in 1M HCl. A series of electrochemical techniques like Open circuit potential (OCP), Electrochemical impedance spectroscopy (EIS), linear polarization resistance (LPR), and potentiodynamic polarization (PDP) were used to analyse the anti-corrosion performance of the nanofiber layer ZnO/NiO/CuO/PCL. The results showed that both anodic and cathodic reactions sharp decline with shift in corrosion potential toward a positive direction in the Tafel plots. LPR results showed that the highest protection efficiency was 94.8% with ZnO-NiO-CuO/PCL nanofiber coating. EIS spectra showed that mild steel coated with ZnO/PCL, NiO/PCL, CuO/PCL, and ZnO-NiO-CuO/PCL, realization of capacitive conduct at high frequency and coating strength at law frequency part with resistor component 474.76 ohm.cm^2, 527.35 ohm.cm^2, 714.73 ohm.cm^2, 744.80 ohm.cm^2 respectively, indicating the good barrier properties and high ohmic resistance of coatings. SEM displayed a straight, interconnected structure, relatively less porosity with uniform fibers diameter. The fibers had average diameter 429 nm, 525 nm, 639 nm, and 443 nm for ZnO/PCL, NiO/PCL, CuO/PCL, and ZnO-NiO-CuO/PCL respectively. EDX and FT-IR results confirmed the existence of ZnO, NiO, and CuO and approved the distribution into PCL matrix. . Results of the present study confirmed that ZnO-NiO-CuO/PCL electrospinning nanfiber coating could be considered as a new metallic oxide nanocomposite coating for a mild steel with excellent corrosion resistance.

1. Introduction

Corrosion of metals still plays a significant role to deterioration the efficiency and losses of the life [1–4]. Tens of billions of damages can be incurred every year by corrosion of steel material [5], as everyone knows. Taking protection on the metal surface is one kind of the economic approach, which can result in avoiding tens of billions of losses per annually [5]. The protective cover of the metal surface is an economically efficient and commonly used form of corrosion prevention [5,6]. Due to their cost-effectiveness, carbon steel is widely used for the construction of marine structures [7]. Steel has been a significant part of our lives because of its comprehensive applications in the automobile, domestic products, company machinery and heavy construction market, such as marine and chemical industries. However, steel corrosion has given us many issues, such as resource loss, breakdown of facilities and environmental pollution [8,9]. Because of the certain mechanical performance and machine strength, mild steel is preferred for infrastructure at low cost and certain time; it should be tried to resist against corrosion occurrences. This reality is among the main triggers of industrial incidents and natural resource use [10]. The most inexpensive and

* Corresponding Author.
E-mail address: mothana.kadhim@qu.edu.iq (M.G.K. AlFalah).

https://doi.org/10.1016/j.surfin.2020.100760
Received 12 August 2020; Received in revised form 2 October 2020; Accepted 12 October 2020
Available online 16 October 2020

Table 1
Polarization data for bare mild steel and coated mild steel with nanofibers film.

Sample	E_{corr} (V)	I_{corr} (μA. cm^{-2})	β_c (V/ dec)	β_a (V/ dec)	LPR_{lp} (ohm. cm^2)	% PE
BLANK	-0.4784	250	0.127	0.105	87	—-
CuO/PCL	-0.4494	41	0.161	0.146	535	83.6
NiO/PCL	-0.4709	21	0.123	0.156	1025	91.6
ZnO/PCL	-0.4754	17.3	0.107	0.136	1254	93.08
ZnO-NiO-CuO/PCL	-0.4681	13	0.121	0.185	1669	94.8

efficient approach for corrosion control nowadays is the application of corrosion resistance coatings on metal surfaces [11–13].

Developing of the surface engineering techniques has made many surface treatments and coatings available for improving the corrosion resistance of metallic materials. Traditional methods such as electrochemical plating [14], electrodeposition [15], anodization [16], or chemical conversion [17] have been the most common methods for this reason, although some include the use of chromates, which present a very significant danger to human safety and the climate. Consequently, to resolve this issue, numerous alternatives are the focus of investigation.

For this reason, the potential to develop and adjust nanoscale materials is an exciting option, because the prospect of incorporating nanoscale texture features on materials will improve the surface to volume ratio and provide an additional functionality [18,19]. It has been shown that the creation of nanostructures against corrosion resistance has been highly effective, utilizing a wide variety of deposition techniques to shield against corrosion of metal substrates including atomic layer deposit [20], spinning coating [21], sol-gel [22], layer-by-layer [23], chemical vapours deposition (CVD) [24] and physical vapour deposit (PVD) [25,26].

Advances in the field of nanotechnology have enabled the manufacture of nanofibers for practical applications with excellent control of their morphology and architectural characteristics. In fact, electrospinning is a technique of growing success in the last few years [27]. It enables the deposition of ultrafine polymeric fibers, even nanometric ones, on metal surfaces [28]. The electrospun fibers can serve as an efficient barrier cover and decrease the metal's corrosion rate. Besides, as a result of their ability to eliminate the corrosion materials and avoid the formation of gas bubbles, porous coatings show greater stability [29,30]. Additionally, the electrospinning method is easy process, versatile, cost-effective, efficient, easy to use and scalable process [31,32] that can be extended to a broad variety of products (natural or synthetic) and can be utilized to increase metal substrates' corrosion resistance. There are several articles on improving the resistive corrosion of coatings using nanofibers such as; PCL [33], PAN-Al_2O_3 [34], polyaniline/poly(methyl methacrylate) PANI/PMMA [35].

Zhao et al. [36] presented experimental implementation of electrospun conducting polyaniline (PANI)/poly(methyl methacrylate) (PMMA) anticorrosion coating film in 3 wt% NaCl solution to protect carbon steel. Results of the tests indicate that electrospun PANI / PMMA microfibers film coated on a carbon steel has improved the efficiency of anticorrosion compared to the PANI / PMMA film drop-cast.

The next innovative method to creating long-term anti-corrosive surfaces is the use of metallic oxide nanocomposites as protective coatings mixed with synthetic polymeric precursors [37]. Kim et al. [38] investigated the using of nanoparticles of zinc oxide (ZnO NPs) incorporated into polymeric precursors such as polycarprolactone (PCL) which deposited onto AZ31 Mg alloys through electrospinning method. They used SEM, EDX, XPS, and FT-IR to characterize PCL / ZnO composite coatings on Mg alloys. The electrochemical corrosion test was carried out to measure the efficiency of coating. The results indicated that the rise in the amount of ZnO nanoparticles in the matrix composites increased the resistance to corrosion. The involvement of ZnO NPs in electrospun fibers can provide additional multifunctionality as an excellent corrosion inhibitor and other benefits which involve antibacterial products, nontoxicity and action against cancer [32]. Karthega et al. [40] explored the composite nanofiber polycaprolactone (PCL) and polycaprolactone / TiO_2 with various weight percentage compositions (2%, 4%, and 6%) of TiO_2 coated over AM50 alloy through electrospinning technique. They utilized surface morphology and elemental composition tests such as SEM, EDX, and FT-IR to investigate the presence of PCL/TiO_2 on the surface of AM50 alloy. The electrochemical technique was used to study the corrosion behaviour of PCL and PCL/TiO_2 coated on AM50 alloy after immersion in a simulated body fluid (SBF) solution. The results exhibited that the rise in the weight percentage of TiO2 enhanced the corrosion resistance as well as a good support for cell proliferation. Bakhsheshi-Rad et al. [41] presented compact nanofiber porous layers of Ta_2O_5 (tantalum pentoxide) and PCL / MgO-Ag (poly (caprolactone)/magnesium oxide-silver) subsequently imposed on Mg alloys by reacting magnetron sputtering and electrospinning to improve anticorrosion as well as antibacterial performance, respectively. PCL / MgO-Ag nanofibers coated through electrospinning were porous, smooth as well as precise, with no recognizable dots. In situ corrosion experiments showed that the nanofiber-coated alloy PCL / MgO-Ag had better corrosion resistance than a Ta_2O_5 sputter-coated alloy or uncoated Mg alloy. To the best of authors' knowledge, the fabrication PCL/ZnO-NiO-CuO coating through electrospinning technique has not been reported yet.

In this study, PCL/ZnO (polycaprolactone/ zinc oxide), PCL/NiO (polycarprolactone/nickel oxide), PCL/CuO (polycarprolactone/copper oxide), and PCL/ZnO-NiO-CuO (polycarprolactone/ zinc oxide- nickel oxide- copper oxide) were fabricated and deposited onto a mild steel through an electrospinning technique. The aim of the present work is to evaluate the effects of electrospun composite nanofiber coatings on a mild steel and also to suppress the mild steel corrosion at 1 M HCl. The behaviour of corrosion was evaluated by means of open circuit potential (OCP), electrochemical impedance spectroscopy (EIS), linear polarization resistance (LPR), and potentiodynamic polarization (PDP) respectively. The surface structure and morphology of the sheet PCL / ZnO, PCL / NiO, PCL / CuO and PCL / ZnO-NiO-CuO coatings have been identified by scanning electron microscope (SEM), energy dispersive X-ray spectroscopy (EDX), and Fourier transform infrared spectroscopy (FT-IR).

2. Materials and methods

2.1. Materials

Cylindrical samples were prepared from a mild steel rod with

Table 2
Impedance spectroscopy data for bare mild steel and coated mild steel with nanofibers film.

Sample	R_S (ohm.cm^2)	R_1 (ohm.cm^2)	CPE_1 (μF.cm^{-2})	n_1	R_2' (ohm.cm^2)	CPE_2 (μF.cm^{-2})	n_2	R_p (ohm.cm^2)	% PE
BLANK	2.5	58	102	0.86	——	——		58	—-
CuO/PCL	4.7	57.77	72	0.70	416.99	67.77	0.79	474.76	88
NiO/PCL	2	78.73	57.83	0.76	448.62	53.75	0.86	527.35	89
ZnO/PCL	2.6	94.43	45.03	0.83	620.30	51.08	0.74	714.73	92
ZnO-NiO-CuO/PCL	0.9	118.22	14.52	0.85	626.58	42.92	0.84	744.80	92.3

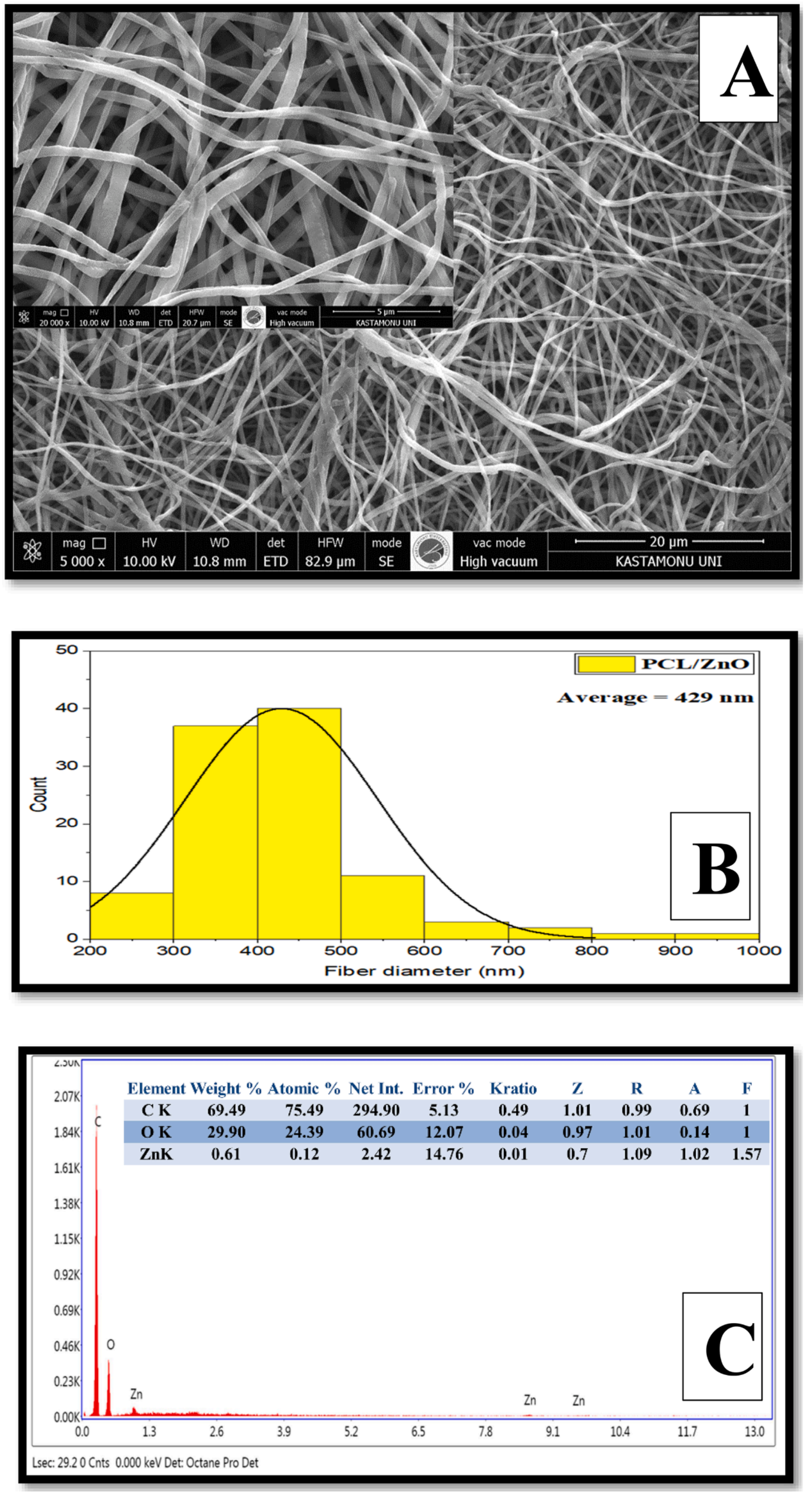

Fig. 1. SEM image for nanofiber film ZnO/PCL (A), diameter distribution (B), and EDX analysis for nanofiber film ZnO/PCL (C).

dimensions (1cm in diameter and 3cm in length) and having a chemical composition (wt. %) 0.18 C, 1.018 Si, 0.0556 Cr, 0.699 Mn, 0.0853 Ni, 0.0939 Cu, and Fe balance. The substrates were connected by copper wire from back and then put it in an epoxy resin with an exposed area of 0.785 cm^2. The samples were polished with silicone carbide up to 2400. The chemical compounds used in the present work were Zinc acetate dehydrate (CH3COO)2Zn•2H2O), Nickel(II) acetate tetrahydrate (Ni (OCOCH3)2•4H2O), Copper(II) acetate hydrate (Cu(CO2CH3)2•H2O), polycaprolactone (PCL, Mw = 80,000 gr/mol), Dichloromethane (DCM) and Methanol. All of them were bought from Sigma-Aldrich Company, USA

2.2. Electrospinning installation and preparation of PCL / ZnO-NiO-CuO coatings

The electrospinning solution (10 wt. %) to produce PCL/ZnO coating was prepared by dissolving 1g PCL in 7ml DCM mixing with 3ml methanol, and then dropped slowly into a solution containing 0.02g zinc

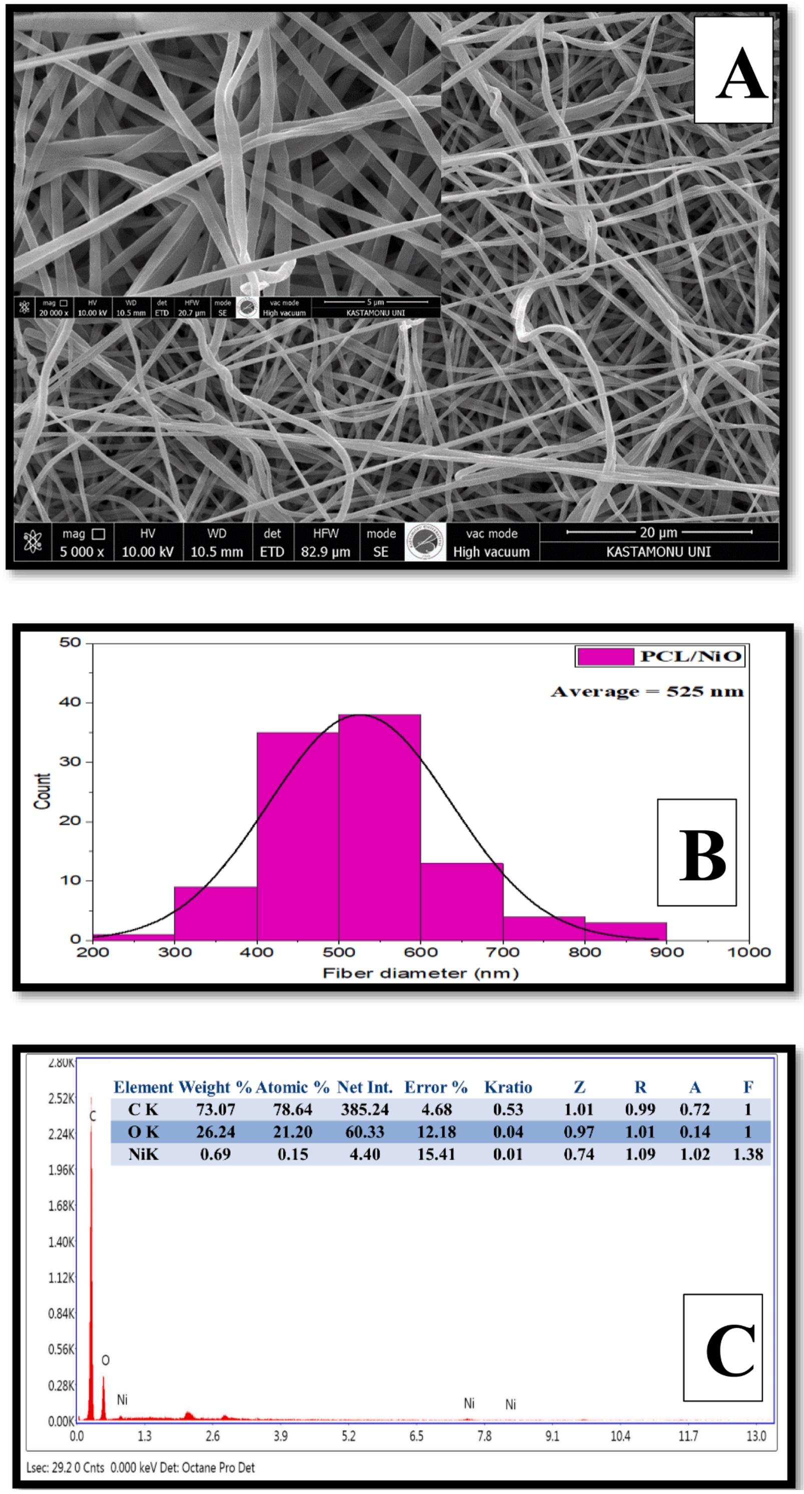

Fig. 2. SEM image for nanofiber film NiO/PCL (A), diameter distribution (B), and EDX analysis for nanofiber film NiO/PCL (C).

acetate and 3ml methanol. Magnetic stirring was applied for 5 h at room temperature to obtain a homogenous solution. The same procedure was repeated to produce PCL/NiO and PCL/CuO coatings by replacing zinc acetate with nickel acetate and copper acetate respectively. In order to produce PCL/ZnO-NiO-CuO, 1g PCL (10 wt. %) was dissolved in 7ml DCM and 3ml methanol with stirring, and then dropped slowly into a solution containing 0.02g zinc acetate, 0.02g nickel acetate, 0.02g copper acetate and 3ml methanol with continuing with magnetic stirring for 6h at room temperature to obtain a homogenous solution. Then, as prepared solutions (PCL / ZnO, PCL / NiO, PCL / CuO, PCL / ZnO-NiO-CuO) for electrospinning coating, 10 ml of needles was packed, and linked via a plastic tube to a copper nozzle (di=1 mm). The solution included a copper nozzle connected to a high-voltage generator. A 20 kV voltage [42,43] was applied to the solution and a dense fibers web on the mild steel was deposited. Electrospinning was performed at a temperature of 20°C with adjusted humidity 30%, flow rate set at 0.01mL/min, and a distance of 12cm from nozzle to the electrode. For this research, the duration of time for coating through electrospinning operation was 5

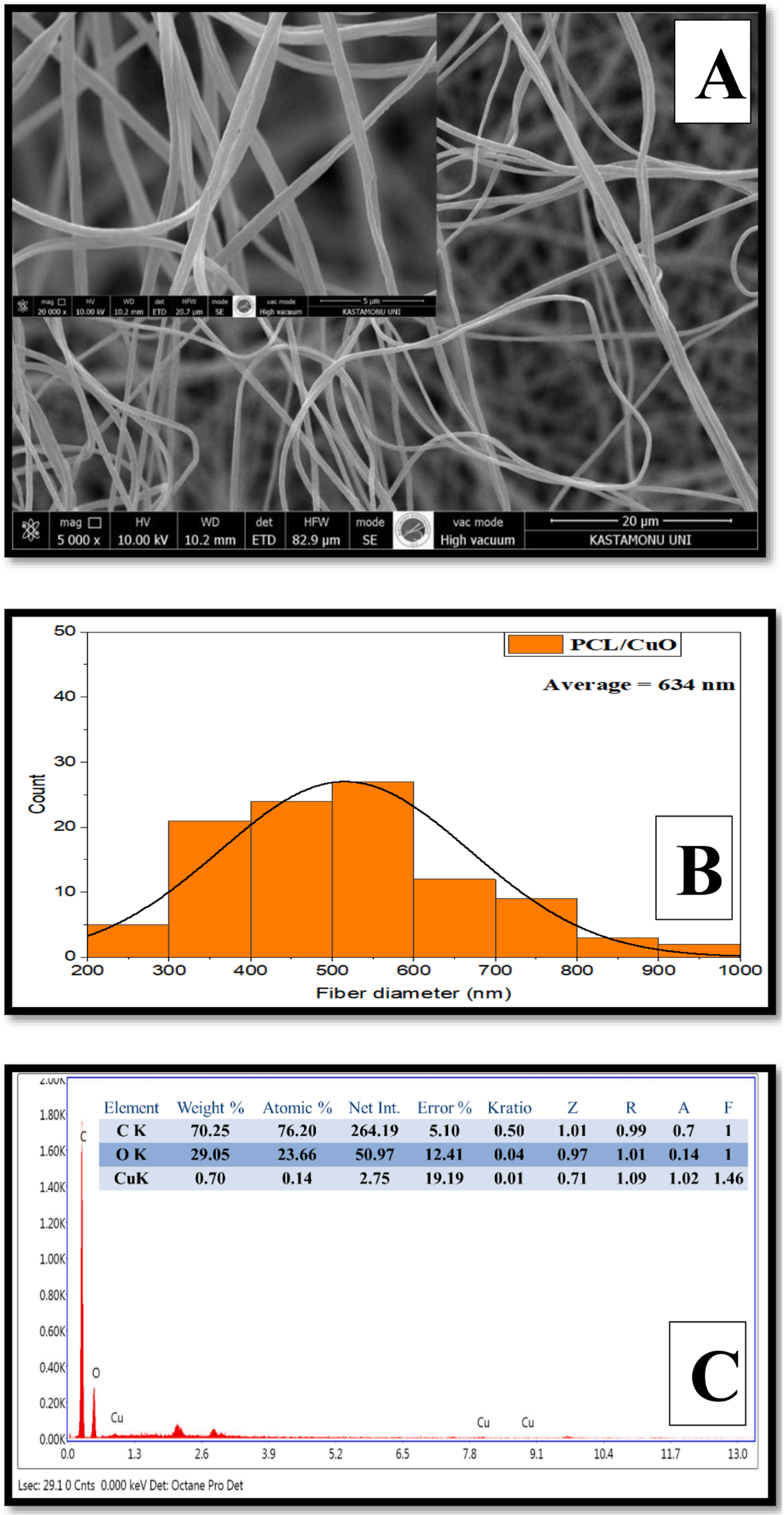

Fig. 3. SEM image for nanofiber film CuO/PCL (A), diameter distribution (B), and EDX analysis for nanofiber film CuO/PCL (C).

minutes for all specimens.

2.3. Electrochemical corrosion tests

The electrochemical experiments were conducted using the a potentiostat (CompactStat Electrochemical Interface, Ivium Technologies, Instrument: B08024, Software: 2699(699)). Three electrode systems; mild steel, Ag/AgCl and platinum wire were used as working electrode, reference electrode, and counter electrode respectively. For this research the acidic solution used was 1M HCl solution. AC electrochemical method such as impedance spectroscopy (EIS), and DC methods such as linear polarization resistance and potentiodynamic polarization as well as open circuit potential (OCP) were utilized in this study. The specimens were immersed in 1 M HCl stagnant solution at

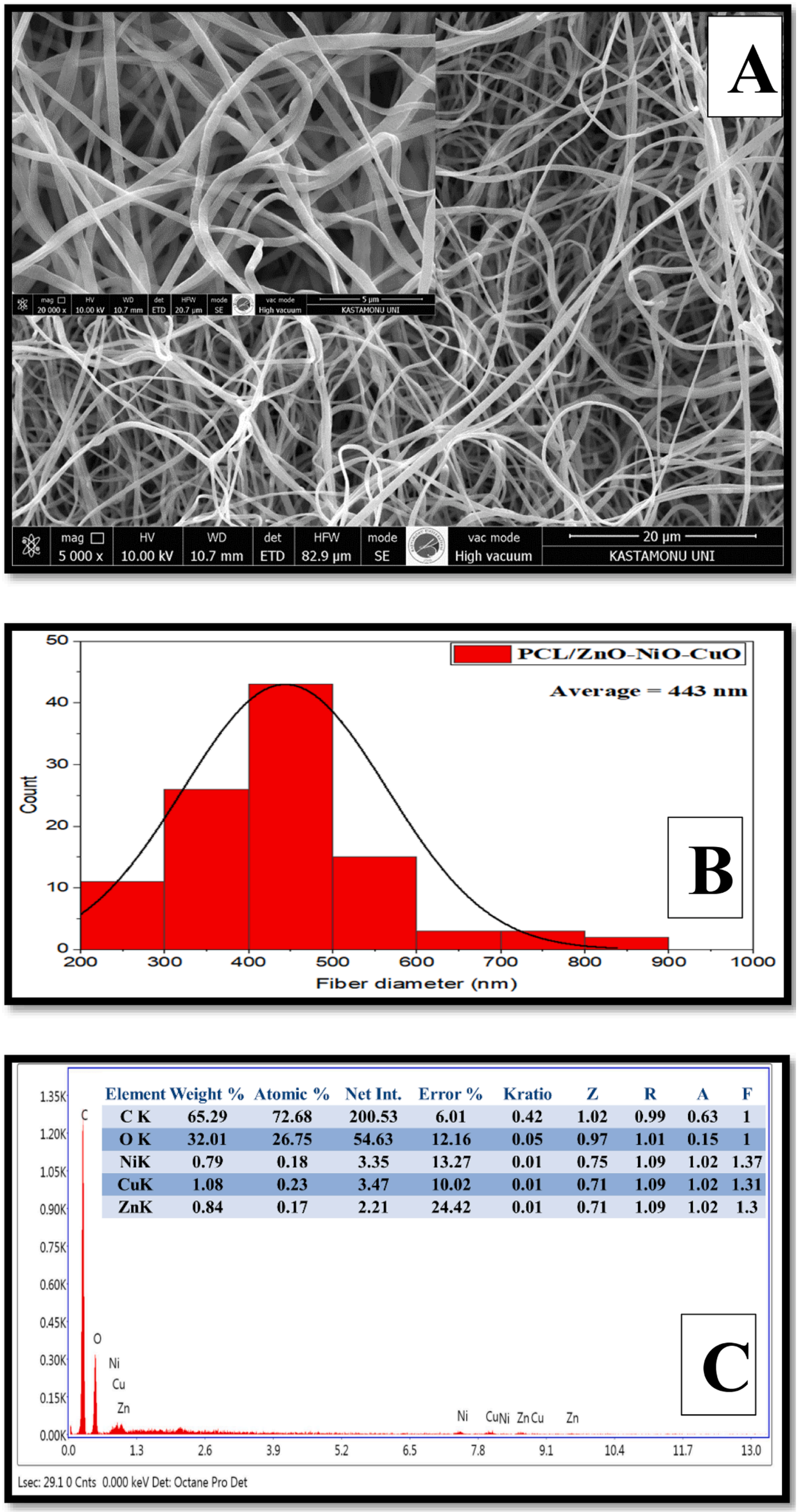

Fig. 4. SEM image for nanofiber film ZnO-NiO-CuO/PCL (A), diameter distribution (B), and EDX analysis for nanofiber film ZnO-NiO-CuO/PCL (C).

room temperature for one hour in order to reach a stable surface state. Impedance spectroscopy (EIS) followed linear polarization resistance (LPR) and then potentiodynamic polarization (PDP) curves have been created. The EIS parameters were measured starting from high frequency 100000 Hz to low frequency 0.01 Hz with an amplitude of 0.005V. The LPR measurements were conducted ± 10 mV as relate to open circuit potential at 60mV / min scan rate starting from cathodic potential to anodic direction, while the PDP measurements were performed ± 250 mV as relate to open circuit potential (OCP) at 60mV / min scan rate. To ensure reproducibility all the electrochemical experiments for each substance was repeated at least three times. The standard deviation for all parameters presented in Table 1 and Table 2 was less than 4%. All curves in this work were fitted to 1cm^2.

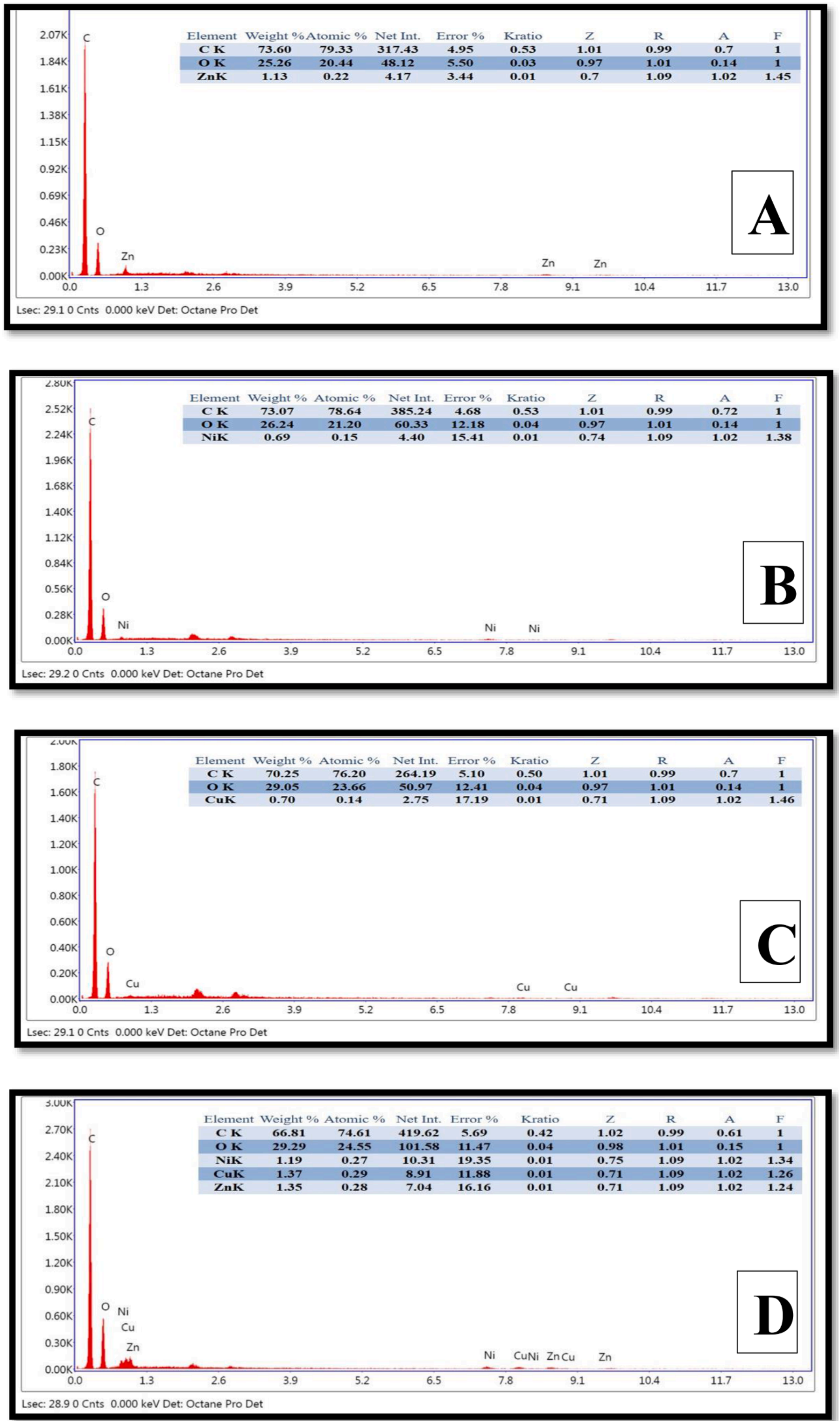

Fig. 5. EDX analysis for spot fiber, A) nanofiber ZnO/PCL, B) nanofiber NiO/PCL, C) nanofiber CuO/PCL, D) nanofiber ZnO-NiO-CuO/PCL.

2.4. Characterization

Scanning electron microscopy (FEG 250 SEM (FEI-Quanta, Hillsboro, OR, USA) has been utilized to examine the surface structure of the various coated mild steel samples. The measurement parameters were: Accelerating voltage (HV) =10 KV, HFW= 20.7μm and 82.9μm, detector= ETD, mode=SE, HIGH VACUME MODE). All samples before being displayed on SEM device were coated with gold-palladium coating, the gold rate is 40% and the palladium rate is 60% for 60 seconds under 40 mA current by using Quanta FEG 250 model of the FEI brand. The surface elemental compositions were analysed through energy dispersive x-ray spectroscopy (EDX). ImageJ technique (Fiji Is just) has been used to estimate the size of fiber and evaluate fiber distribution. Fourier-transform infrared spectroscopy (FT-IR), (Bruker model-ALPHA) was conducted to examine the difference in the chemical components of the coatings.

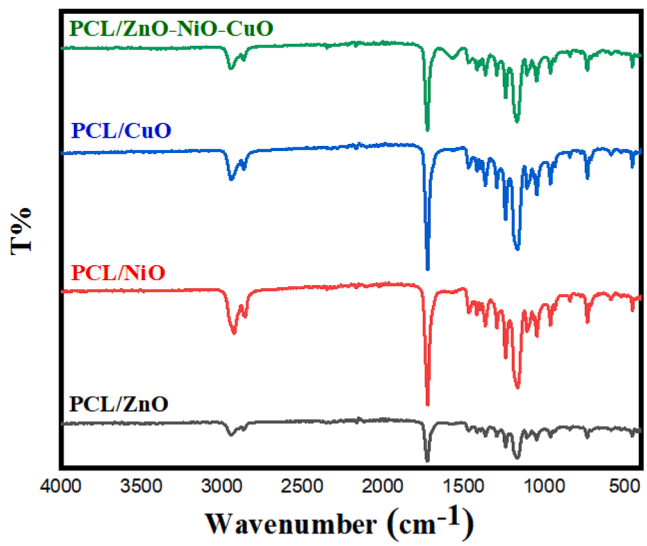

Fig. 6. FT-IR spectra of PCL/ZnO, PCL/NiO, PCL/CuO, and PCL/ZnO-NiO-CuO nanofiber film.

3. Results and Discussion

3.1. SEM and EDX characterization

Figs. 1–4 display the descriptive SEM images and EDX results of the composite coatings ZnO / PCL, NiO / PCL, CuO / PCL and ZnO-NiO-CuO / PCL on the mild steel respectively. In general, the nanofibers for all composite coatings exhibited a straight and interconnected structure with uniform diameter. A dense structure of entangled threads and thinner diameter with slight agglomeration as can be seen in Fig. 1 (A). A similar behaviour can be seen in Fig. 4 (A) with an increase in the roughness of fibers due to the presence of ZnO, NiO, and CuO in PCL matrix. A thicker diameter with wrapped nanofibers can be seen in Fig. 2 (A), while in Fig. 3 (A), it can be seen that the diameter become thicker with a layer more porosity comparing with other coatings.

Mean fiber diameters and fiber distribution of ZnO / PCL, NiO / PCL, CuO / PCL, and ZnO-NiO-CuO / PCL nanofibers have been collected through examination of at among at 105 fibers utilizing the Fiji Image J software as shown in Figs. 1–4(B). Variations in the viscosity and conductance of electrospinning solutions have shown the fiber shape, fiber diameters and size distributions are being differed [31,44,45]. Although the morphological characteristics of each electrospun solution were noticeably different in the present study, the mean diameter showed values such as 429 nm, 525 nm, 634 nm, and 443 nm for ZnO / PCL, NiO / PCL, CuO / PCL, and ZnO-NiO-CuO / PCL, respectively. The distribution of diameters clearly showed that the layers of ZnO / PCL and ZnO-NiO-CuO / PCL generate fibers that are more regular than NiO / PCL and CuO / PCL.

The EDX analysis has also been utilized to identify the influence of ZnO, NiO, and CuO on morphological features as shown in Figs. 1–4(C). The findings display differing atomic percentage of the composite coatings ZnO / PCL, NiO / PCL, CuO / PCL, and ZnO-NiO-CuO / PCL on the mild steel substrate surface. The EDX spectrum of ZnO / PCL, NiO / PCL, CuO / PCL, and ZnO-NiO-CuO / PCL composite samples showed the existence of ZnO, NiO, CuO, and approved the distribution of ZnO, NiO, and CuO in the fibers. The various chemical composition (in percent) of electrospun coated specimens also refers that the quantity of ZnO, NiO, CuO may directly impact the porosity, the pore size and the roughness of nanofibrous surfaces [46]. It can be seen clearly in Fig. 4(C), that the chemical composition of O element was increased significantly due to the presence of Zn, Ni, Cu in the PCL fibers. In order to provide a strong evidence to the presence of ZnO, NiO, CuO in PCL fibers, EDX analysis was used as shown in Fig. 5(A-D) for individual fiber in ZnO / PCL, NiO / PCL, CuO / PCL, and ZnO-NiO-CuO / PCL composite coatings on mild steel respectively.

3.2. FT-IR characterization

In order to discover a difference in the chemical structure from an electrospinning coating technique, FT-IR spectrum was collected in the wavenumber range of 400-4000 cm^{-1}. Fig. 6 reveals PCL / ZnO, PCL / NiO, PCL / CuO and PCL / ZnO-NiO-CuO composite coatings on a mild steel surface. In the PCL/ZnO coating, the peaks are shown at 2945.90 and 2867.26 cm^{-1} which corresponded to the C-H of saturated carbons. The –CO stretching in ester carbonyl group from PCL polymer is observed at 1724.95 cm^{-1} [39,45,47]. The peak at 1470.75 cm^{-1} is related to the bond C-H scissoring, while the peak at 1168 cm^{-1} is related to the C- O - C [47]. The peak at 1047 cm^{-1} is related to the stretching CO – O – CO. The peaks at range 400 - 596 cm^{-1} are related to Zn – O bond which is in agreement with previous studies [42,48]. In the PCL/NiO coating, the peaks of C-H, –CO were shifted to a lower

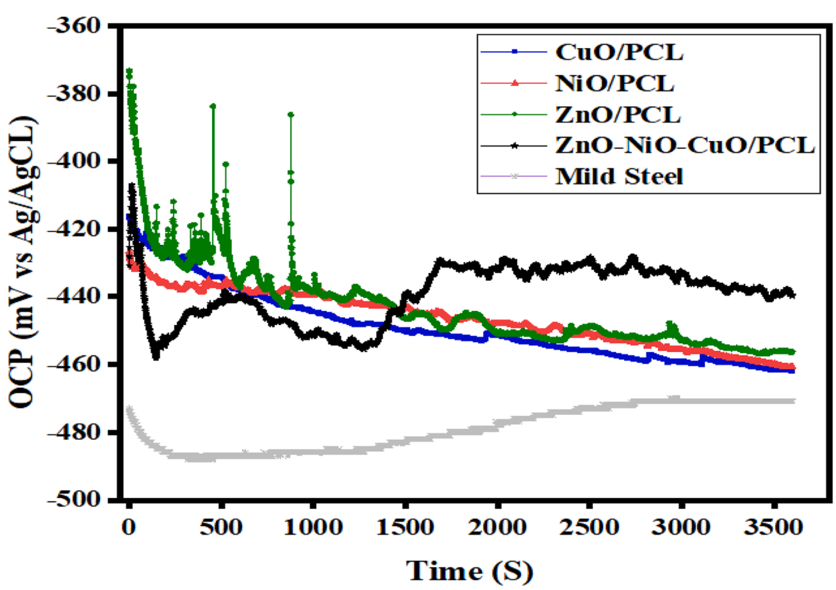

Fig. 7. Open circuit potential curves (OCP) for bare mild steel and coated mild steel with nanofibers film in 1M HCl.

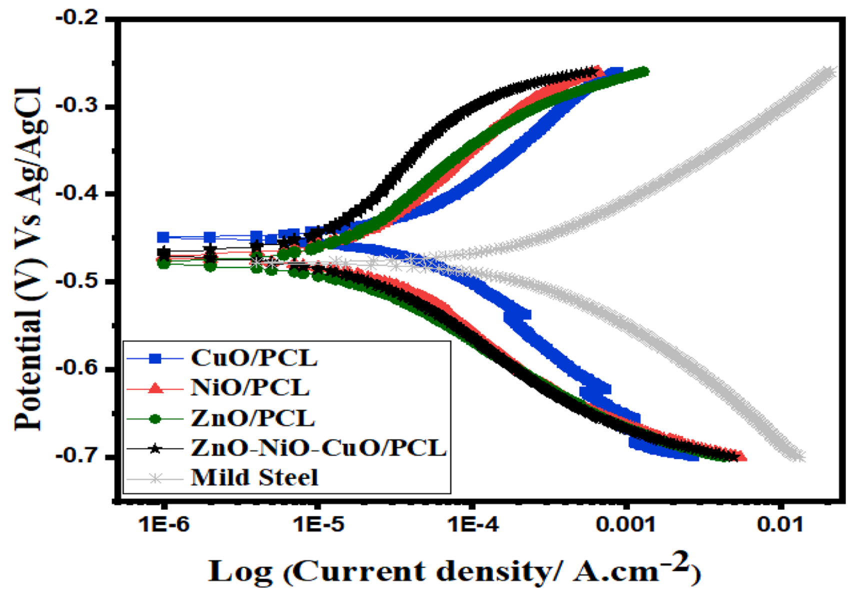

Fig. 8. Potentiodynamic polarization curves for bare mild steel and coated mild steel with nanofibers film in 1M HCl.

wavenumber of 2924.59, 2856.56, 1722.86 cm^{-1} respectively. Similar phenomena were observed with the peaks of C-H scissoring, C- O – C, CO – O – CO. This may be because of the formation of hydrogen bonds between NiO and PCL [49]. The peaks at range 400 – 452 cm^{-1} may relate to Ni – O bonds [43]. In the PCL/CuO coating, similar phenomena were observed with the peaks C-H, –CO, which were slightly shifted to a lower wavenumber of 2942.84, 2865.24, 1722.93 cm^{-1}. The peaks at range 500 – 584.83 cm^{-1} may relate to Cu – O bonds [50]. The PCL/ZnO-NiO-CuO composite displays almost identical characteristic peaks of PCL/ZnO, PCL/NiO, and PCL/CuO. Compared with PCL/ZnO, the peaks C-H, –CO were shifted slightly to lower wavenumber 2943.75, 2866.93,1724.63 cm^{-1}.The new peak is observed at 1572.73 cm^{-1}, which corresponded to the C= C cyclic alkene. The peaks at range 420-583 cm^{-1} may relate to Zn – O, Ni – O, Cu – O [51].

FT-IR spectrum for pure PCL coating was reported in many researches [38,39,45,47,48] when compared to the PCL / ZnO, PCL / NiO, PCL / CuO and PCL / ZnO-NiO-CuO coatings showed a significant change in the transmittance peaks for all coatings thus providing an evidence that ZnO, NiO, CuO layers have been interacted into PCL matrix.

3.3. Corrosion tests

3.3.1. Open circuit potential (OCP), Potentiodynamic polarization (PDP) and linear polarization resistance (LPR) tests

Fig. 7 shows OCP vs. time (immersion time 1h) curves for mild steel, coated mild steel with CuO/PCL, coated mild steel with NiO/PCL, coated mild steel with ZnO/PCL, and coated mild steel with ZnO-NiO-CuO/PCL in 1M HCl solution. It can be seen that the OCP for the mild steel started from -0.475 V and OCP shifted to negative value -0.488 V within few minutes due to the occurrence of a general corrosion on the surface of the mild steel. However, the OCP attained the steady state with a value of -0.471 V after 1h of immersion. In case of a mild steel coated with CuO/PCL, the OCP started with -0.416 V and decreased gradually towards more negative value until arrived to the steady state with a value -0.461 V after 1h. This is could be due to start of diffusion of aggressive ions such as hydrogen and chloride through the coating. Similar behaviour with a slightly difference can be seen for a mild steel coated with NiO/PCL, the OCP started with a value of -0.425 V until arrived to the steady state with a value of -0.460 V. Interesting results were noticed for ZnO/PCL and ZnO-NiO-CuO/PCL coatings. In case ZnO/PCL coating, the OCP started from -0.373 V and shifted sharply with fluctuated to more negative potential within few minutes of immersion. This is may be due to rapid diffusion of hydrogen or chloride ions through the coating. Thereafter, the OCP reached a steady state value of -0.456 V at end of immersion time. While a four stage OCP variation were observed for ZnO-NiO-CuO/PCL coating. The OCP started from -0.40 V and shifted sharply to negative potential within few minutes of immersion with a value of -0.45 V followed by a sharply shifting toward more positive potential with a value of -0.439 V. Thereafter, the OCP shifted again to the negative potential with the increasing of time followed by shifting again toward more positive potential until reached the steady state with a value of -0.43 V at end of immersion. The positive move in OCP essentially indicates the passive condition of underlying metal due to the surface film's good corrosion resistance capability. The highly positive OCP values are attributed to the productive role of ZnO-NiO-CuO / PCL composite for the inhibition of aggressive ions such as hydrogen and chloride in the surface of the metal [6,52].

Fig. 8 shows PDP curves for mild steel, coated mild steel with CuO/PCL, coated mild steel with NiO/PCL, coated mild steel with ZnO/PCL, and coated mild steel with ZnO-NiO-CuO/PCL in 1M HCl solution. All electrochemical parameters for PDP and LPR, such as protection efficiency PE (see Eq. (1)), corrosion current density I_{Corr}, corrosion potential E_{Corr}, anodic Tafel slopes and cathodic Tafel slopes β_a & β_c, linear polarization resistance LPR are listed in Table 1. It can be noted from Table 1 that the values of protection efficiency PE for CuO/PCL, NiO/PCL, ZnO/PCL, and ZnO-NiO-CuO/PCL coatings are 83.6%, 91.6%, 93.08%, and 94.8% respectively. These results means that all coatings provide a strong protection against the corrosion. The electrospun ZnO-NiO-CuO/PCL film appears to be better than CuO/PCL, NiO/PCL, and ZnO/PCL. Moreover, corrosion current density decreased sharply from 250 μA.cm^{-2} to 13 μA.cm^{-2} with coated ZnO-NiO-CuO/PCL. Furthermore, it can be seen clearly from Fig. 7 that both anodic and cathodic curves were remarkably shifted towards less current density attributed to the existence of a fairly compact coating which making it far more difficult to transfer violent ions and penetration to the metal surface hence more powerful shielding barrier to the corrosion of mild steel. However, for anodic protection, the irregular shifts of the E_{Corr} of the mild steel coated ZnO/NiO/CuO/PCL film suggest that various anti-corrosion mechanism occur for each coating. Compared to mild steel without coating, the positive shift of the E_{Corr} of ZnO/PCL,NiO/PCL, CuO/PCL, and ZnO-NiO-CuO/PCL coated on the mild steel suggests the presence of passivation layer [53]. The appearance of passivation layer on the respective four coatings has to do with the near relation between

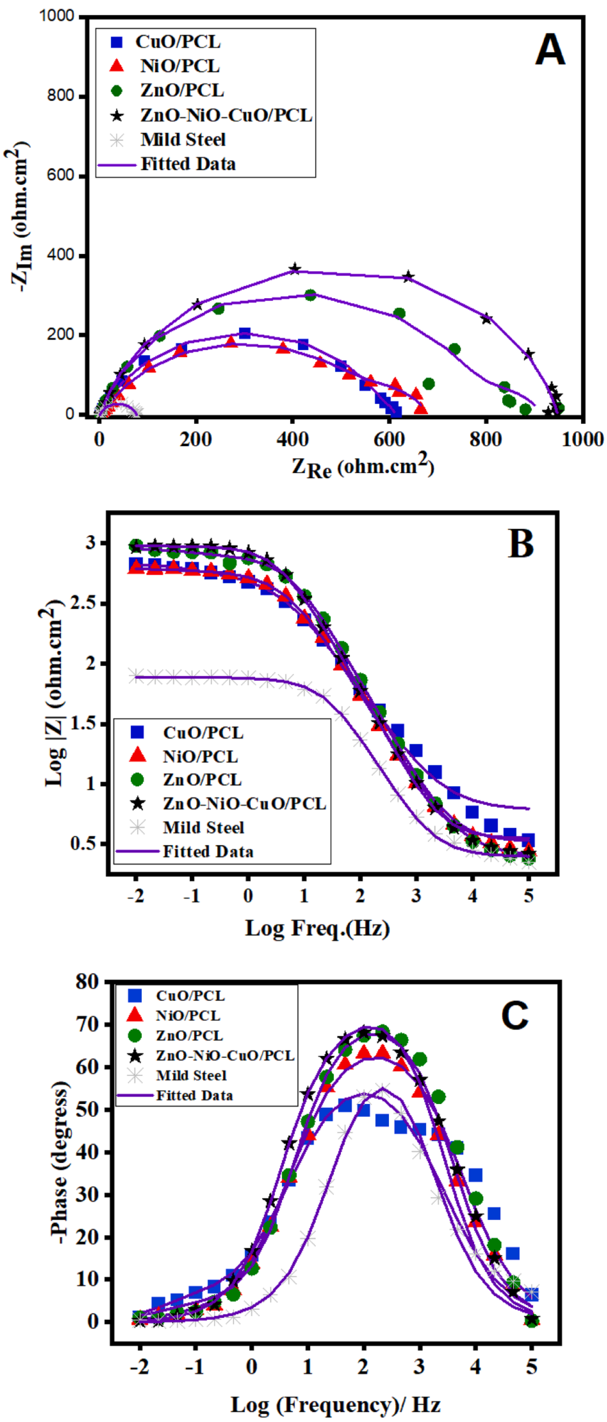

Fig. 9. Nyquist plots for mild steel and coated mild steel with nanofibers film in 1M HCl (A), Bode magnitude plots for mild steel and coated mild steel with nanofibers film in 1M HCl (B), and Bode phase angle plots for mild steel and coated mild steel with nanofibers film in 1M HCl (C).

the coating and the mild steel substrate. The passivation layer, that concerns with high stability and oxidation / reduction conducting polymers chemistry, allows it possible to preserve the equilibrium in the passivation region resulting in a substantial decrease in the speed of corrosion [54,55].

On the other hand, results of LPR shown in Table.1, confirm that the resistance polarization follows an order ZnO-NiO-CuO/PCL ˃ ZnO/PCL ˃ NiO/PCL ˃ CuO/PCL ˃ mild steel, which is contrary to corrosion current density. This implies the I_{Corr} is directly proportional to the values of 1/ R_{LPR}.

Eq. (1) can be used to measure the protection efficiency [56].

$$\%PE = [1 - I_{Corr} / I_{UnCorr}] \times 100 \quad (1)$$

Where, I_{UnCorr}, I_{Corr} refer to uncoated and coated corrosion current density respectively.

3.3.2. Electrochemical impedance spectroscopy tests

The EIS plots, as seen in Fig. 9 (A) – (C), have been obtained to explore the mechanisms of corrosion on the electrode / electrolyte interface. It can be seen from Fig. 9(A), the Nyquist plot for the mild steel without coating contain at high frequency depressed semicircle due to the roughness and inhomogeneity of the surface, whereas at low frequency it contains an inductive loop due to the adsorption of an intermediate component in the corrosion reaction [57] . Additionally, Fig. 9 (A) displays other four EIS spectra of mild steel coated with ZnO / PCL, NiO / PCL, CuO / PCL, and ZnO-NiO-CuO / PCL, showing semicircle but their diameter obviously are varying and becoming bigger. It is well understood that the appearance of the semicircle forms in Nyquist plots describes not only the resistance to transfer charging, but also the capacitance of the double electrical layer between the substrate and the electrolyte interface [58]. Moreover, from Fig. 9(A) in comparison with non-coating of mild steel specimens, the coated specimens recorded high universal impedances which demonstrated an improvement in the barrier property anti corrosion in the coated specimens. Furthermore, the ZnO-NiO-CuO / PCL coated sample provided the largest diameter which strongly suggests the highest resistance to corrosion among the coated samples. A new evident can be seen from Fig. 9(B)–(C), Bode magnitude plots and Bode phase angle plots for mild steel and coated mild steel with nanofibers film in 1M HCl, respectively. It is well known that the parameters for determining the corrosion resistance of the coating are both the impedance modulus (|Z|) at low frequency and the phase angle at high frequency [38]. In Fig. 9(B), the value of impedance modulus |Z| of the four mild steel samples coated with nanofibers film are higher than that of mild steel sample without coating, indicates outstanding efficiency of barriers to corrosive media diffusion by coating. Moreover, it can be seen from Fig. 9(C), that the phase angle at high frequency for the mild steel coated with ZnO-NiO-CuO / PCL is around 70^{o} higher than mild steel without coating, confirming better interfacial contact with mild steel coated with nanofibers film [56]. On the other words, the best coating was ZnO-NiO-CuO / PCL coated on mild steel when compared to others three coatings.

All the EIS values of uncoated and coated mild steel parameters extracted with Ivium Technologies, Instrument: B08024, Software:2699 (699) by fitting EIS plots described in Table 2. The protection efficiency (PE) was calculated by used Eq. (2) [13,59] and summarized in Table 2 as well.

$$\%PE = \left(R_P - - R_P{}^{O} / R_P\right) \times 100 \quad (2)$$

Where, Rp and $R_P{}^{\circ}$ coated and uncoated polarization resistance respectively.

Fig. 10 (A and B) show the equivalent circuit for uncoated and coated mild steel with electrospun ZnO/NiO/CuO/PCL respectively. In this case CPE is a constant phase element, n is a phase shift which is represented as a uniformity level of the substrate [60]. To give a more precise match to the experimental tests, CPE was utilized in place of a double layer capacitance (C_{dl}) [61,62]. The model of the equivalent circuit diagram in Fig. 10(A), resistance of solution (R_S), polarization resistance (R_P) = transmission of resistance charge (R_{CT}) + diffuse layer resistance (R_d) + accumular material resistance (corrosive materials, some present molecules or ions) (Ra). At the model in Fig. 10(B), R_1 is film resistance, R_2 = film resistance (R_f) + resistance referring to unprotected areas and pores (R_{por}), R_{por} = R_{CT} + R_d + R_a, and R_p = R_1 + R_2. CPE_1 is the capacitance of films (Cf) can be calculated according to Eq. (3), while in case CPE_2 is the capacitance of double layers (Cdl) can be calculated

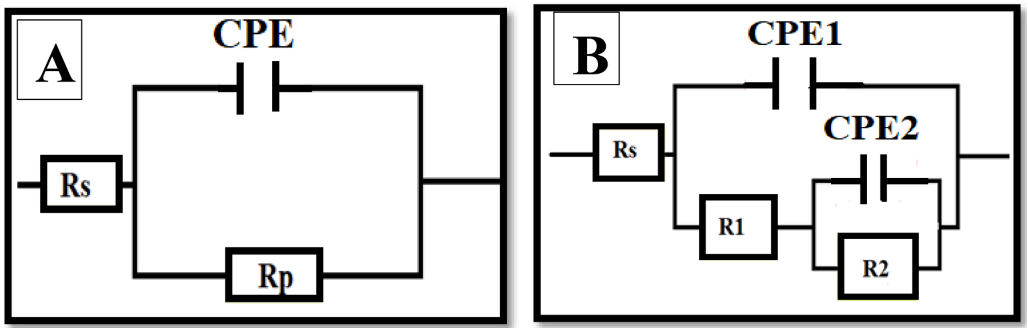

Fig. 10. Equivalent circuit model for mild steel in 1M HCl (A), and Equivalent circuit model for mild steel coated with nanofiber film in 1M HCl (B).

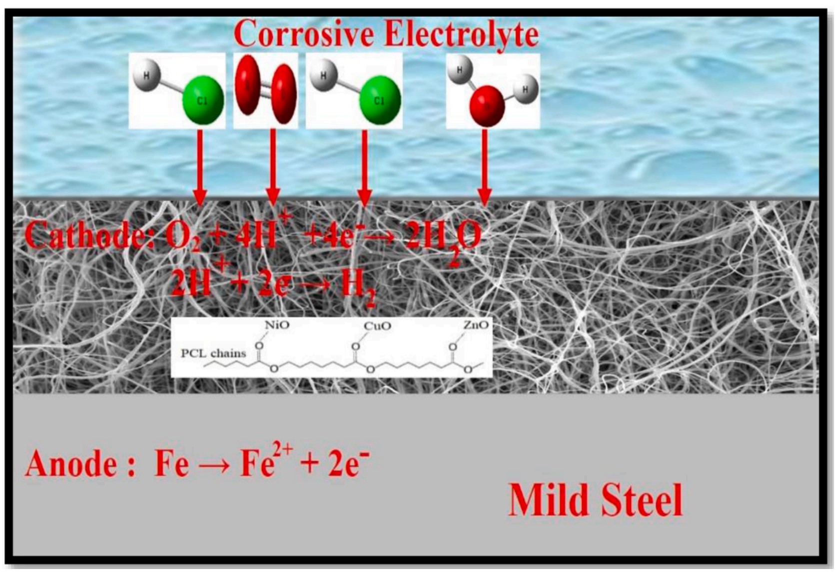

Fig. 11. Schematic the plausible mechanism of corrosion for PCL/ZnO-NiO-CuO coatings on mild steel in 1M HCl.

according to Eq. (4) [63].

$$C_f = \left(Q_1 \times R_1{}^{1-n}\right)^{1/n} \tag{3}$$

$$C_{dl} = \left(Q_2 \times R_2{}^{1-n}\right)^{1/n} \tag{4}$$

Where, Q_1 and Q_2 refer to the film capacitance and the double layer capacitance respectively [63].

The protection efficiency follows an order ZnO-NiO-CuO/PCL ˃ ZnO/PCL ˃ NiO/PCL ˃ CuO/PCL.

The Open circuit potential (OCP), potentiodynamic polarization (PDP), linear polarization resistance (LPR), and electrochemical impedance spectroscopy (EIS) experiments show that anticorrosion performances of the electrospun ZnO-NiO-CuO/PCL film to the mild steel is better than those ZnO/PCL, NiO/PCL, CuO/PCL coated on mild steel.

3.4. Anti corrosion mechanism

The plausible mechanism of corrosion, it may be clarified as follows. The anodic reaction is the dissolution of mild steel in the corrosion process and the subsequent formation of Fe^{2+} ions. In the case of cathodic process, oxygen reduction and H^+ are diffused to PCL / ZnO-NiO-CuO or mild steel, and H_2 is released to PCL / ZnO-NiO-CuO coating or mild steel surface (see Fig. 11). The medium-permeability resistance can inhibit H^+ ion and H_2O absorption, hence H_2 production during the reactions [54,55]. Consequently, it is worth noting that the released H_2 gas occupied in the holes will obstruct H^+ diffused to the metal surface. In addition, the H_2 gas in the holes can also reduce the diffusion of anode-generated Fe^{+2} ions by PCL / ZnO-NiO-CuO coatings into the HCL solution [6,64]. Hence good resistance to permeability will delay the corrosion reaction as well as provide stronger protection against corrosion for metals. In other words, PCL / ZnO-NiO-CuO coatings provides an efficient protection for the anodic processes.

4. Conclusion

In the present work, fabrications, characteristics, and corrosion studies of electrospinning nanofibers ZnO/PCL, NiO/PCL, CuO/PCL, and ZnO-NiO-CuO/PCL coatings on a mild steel surface were performed successfully. The results confirmed that ZnO-NiO-CuO/PCL electrospinning nanfiber coating could be considered as a new layer of corrosion protective coating for mild steel with excellent corrosion resistance. ZnO-NiO-CuO/PCL and ZnO/PCL nanfiber coatings were found to be more effect on the deposition compared to NiO/PCL and CuO/PCL. SEM results displayed a straight, interconnected structure with less porosity and uniform fibers diameter. The fibers had an average diameter of 429 nm, 525 nm, 639 nm, and 443 nm for ZnO/PCL, NiO/PCL, CuO/PCL, and ZnO-NiO-CuO/PCL respectively. EDX and FT-IR results confirmed the existence of ZnO, NiO, and CuO and approved their uniform distribution into PCL nanfibrous coating. A higher protection efficiency (94.8%) was observed for ZnO-NiO-CuO/PCL coating confirming a strong protection against the corrosion. EIS spectra showed that ZnO/PCL, NiO/PCL, CuO/PCL, and ZnO-NiO-CuO/PCL coatings have resistor component 474.76 ohm.cm^2, 527.35 ohm.cm^2, 714.73 ohm.cm^2, 744.80 ohm.cm^2 respectively, which additionally indicate the high ohmic resistance of coatings.

CRediT authorship contribution statement

Mothana Ghazi Kadhim AlFalah: Conceptualization, Formal analysis, Methodology, Writing - original draft. **Ersin Kamberli:** Methodology, Resources, Writing - original draft. **Ali H. Abbar:** Investigation, Writing - review & editing. **Fatma Kandemirli:** Supervision, Visualization. **Murat Saracoglu:** Writing - review & editing.

Declaration of Competing Interest

We have no conflicts of interest to disclose.

Acknowledgements

The authors gratefully acknowledge Kastamonu University Scientific Research Coordination Unit. Project Number KÜ-BAP 2017-74 for financials support. Mothana Ghazi Kadhim AlFalah also thanks Materials of Engineering department, college of Engineering, University of Al-Qadisiyah, Iraq, for give opportunity to complete his study throughout PhD programme.

References

[1] P.B. Raja, M. Ismail, S. Ghoreishiamiri, J. Mirza, M.C. Ismail, S. Kakooei, A. A. Rahim, Reviews on Corrosion Inhibitors: A Short View, Chem. Eng. Commun 203 (2016) 1145–1156, https://doi.org/10.1080/00986445.2016.1172485.

[2] R. Solmaz, E. Altunbaş Şahin, G. Kardaş, Electrochemical preparation and characterization of nickel and zinc-modified poly-2-aminothiazole films on mild steel surface and their corrosion inhibition performance, React. Funct. Polym 71 (2011) 1148–1154, https://doi.org/10.1016/j.reactfunctpolym.2011.09.002.

[3] S.A. Umoren, U.M. Eduok, Application of carbohydrate polymers as corrosion inhibitors for metal substrates in different media: A review, Carbohydr. Polym 140 (2016) 314–341, https://doi.org/10.1016/j.carbpol.2015.12.038.

[4] V. Karpakam, K. Kamaraj, S. Sathiyanarayanan, G. Venkatachari, S. Ramu, Electrosynthesis of polyaniline-molybdate coating on steel and its corrosion protection performance, Electrochim. Acta 56 (2011) 2165–2173, https://doi.org/10.1016/j.electacta.2010.11.099.

[5] M. Shaterian, A. Khoobi, M. Enhessari, K. Ozaee, A new strategy based on thermodiffusion of ceramic nanopigments into metal surfaces and formation of anti-corrosion coatings, Microporous Mesoporous Mater 218 (2015) 62–68, https://doi.org/10.1016/j.micromeso.2015.06.039.

[6] G. Ruhi, H. Bhandari, S.K. Dhawan, Designing of corrosion resistant epoxy coatings embedded with polypyrrole/SiO2 composite, Prog. Org. Coatings 77 (2014) 1484–1498, https://doi.org/10.1016/j.porgcoat.2014.04.013.

[7] J. Huang, Y. Liu, J. Yuan, H. Li, Al/Al2O3 composite coating deposited by flame spraying for marine applications: Alumina skeleton enhances anti-corrosion and wear performances, J, Therm. Spray Technol. 23 (2014) 676–683, https://doi.org/10.1007/s11666-014-0056-7.

[8] K. Zhu, X. Li, H. Wang, J. Li, G. Fei, Electrochemical and anti-corrosion behaviors of water dispersible graphene/acrylic modified alkyd resin latex composites coated carbon steel, Appl. PolJournalymer Sci 134 (2017) 1–12, https://doi.org/10.1002/app.44445.

[9] M. Stipaničev, F. Turcu, L. Esnault, E.W. Schweitzer, R. Kilian, R. Basseguy, Corrosion behavior of carbon steel in presence of sulfate-reducing bacteria in seawater environment, Electrochim. Acta 113 (2013) 390–406, https://doi.org/10.1016/j.electacta.2013.09.059.

[10] M. Behzadnasab, S.M. Mirabedini, K. Kabiri, S. Jamali, Corrosion performance of epoxy coatings containing silane treated ZrO 2 nanoparticles on mild steel in 3 . 5 % NaCl solution, Corros. Sci. 53 (2011) 89–98, https://doi.org/10.1016/j.corsci.2010.09.026.

[11] T.F.Zhang Wan, J.C. Ding, C.M. Kim, S.W. Park, Y. Yang, K.H. Kim, S.H. Kwon, Enhanced Corrosion Resistance of PVD-CrN Coatings by ALD Sealing Layers, Nanoscale Res. Lett 12 (2017) 1–8, https://doi.org/10.1186/s11671-017-2020-1.

[12] M. Bagherzadeh, H. Haddadi, M. Iranpour, Electrochemical evaluation and surface study of magnetite/PANI nanocomposite for carbon steel protection in 3.5% NaCl, Prog. Org. Coatings. 101 (2016) 149–160, https://doi.org/10.1016/j.porgcoat.2016.08.011.

[13] M. Bagherzadeh, Z.S. Ghahfarokhi, E.G. Yazdi, Electrochemical and surface evaluation of the anti-corrosion properties of reduced graphene oxide, RSC Adv 6 (2016) 22007–22015, https://doi.org/10.1039/c5ra26948b.

[14] R. Cohen, Koch U., F B, Sard, Electroplating of cyclic multilayered alloy (CMA) coatings, J. Electrochem. Soc. 130 (10) (1983) 1987–1995.

[15] R. Solmaz, G. Kardaş, Electrochemical deposition and characterization of NiFe coatings as electrocatalytic materials for alkaline water electrolysis, Electrochim. Acta 54 (2009) 3726–3734, https://doi.org/10.1016/j.electacta.2009.01.064.

[16] F. Mansfeld, M.W. Kendig, Evaluation of Anodized Aluminum Surfaces With Electrochemical Impedance Spectroscopy, Proc. - Electrochem. Soc 86–11 (1986) 263–273.

[17] K.Z. Chong, T.S. Shih, Conversion-coating treatment for magnesium alloys by a permanganate-phosphate solution, Mater. Chem. Phys 80 (2003) 191–200, https://doi.org/10.1016/S0254-0584(02)00481-9.

[18] W. Li, Y. Zong, Q. Liu, Y. Sun, Z. Li, H. Wang, Z. Li, A highly stretchable and biodegradable superamphiphobic fluorinated polycaprolactone nanofibrous membrane for antifouling, Prog. Org. Coatings (2020) 147, https://doi.org/10.1016/j.porgcoat.2020.105776.

[19] J. Yan, P. Xu, S. Chen, G. Wang, F. Zhang, W. Zhao, Z. Zhang, Z. Deng, M. Xu, J. Yun, Y. Zhang, Construction of highly ordered ZnO microrod@SnO2 nanowire heterojunction hybrid with a test-tube brush-like structure for high performance lithium-ion batteries: experimental and theoretical study, Electrochim. Acta 330 (2020), 135312, https://doi.org/10.1016/j.electacta.2019.135312.

[20] C.X. Shan, X. Hou, K.L. Choy, Corrosion resistance of TiO2 films grown on stainless steel by atomic layer deposition, Surf. Coatings Technol 202 (2008) 2399–2402, https://doi.org/10.1016/j.surfcoat.2007.08.066.

[21] T.F. Conceicao, N. Scharnagl, C. Blawert, W. Dietzel, K.U. Kainer, Corrosion protection of magnesium alloy AZ31 sheets by spin coating process with poly(ether imide) [PEI], Corros. Sci 52 (2010) 2066–2079, https://doi.org/10.1016/j.corsci.2010.02.027.

[22] D. Wang, G.P. Bierwagen, Sol-gel coatings on metals for corrosion protection, Prog. Org. Coatings 64 (2009) 327–338, https://doi.org/10.1016/j.porgcoat.2008.08.010.

[23] D.G. Shchukin, M. Zheludkevich, K. Yasakau, S. Lamaka, M.G.S. Ferreira, H. Möhwald, Layer-by-layer assembled nanocontainers for self-healing corrosion protection, Adv. Mater 18 (2006) 1672–1678, https://doi.org/10.1002/adma.200502053.

[24] T. Ishizaki, J. Hieda, N. Saito, N. Saito, O. Takai, Corrosion resistance and chemical stability of super-hydrophobic film deposited on magnesium alloy AZ31 by microwave plasma-enhanced chemical vapor deposition, Electrochim. Acta 55 (2010) 7094–7101, https://doi.org/10.1016/j.electacta.2010.06.064.

[25] H.A. Jehn, Improvement of the corrosion resistance of PVD hard coating-substrate systems, Surf. Coatings Technol 125 (2000) 212–217, https://doi.org/10.1016/S0257-8972(99)00551-4.

[26] G. Bertrand, H. Mahdjoub, C. Meunier, A study of the corrosion behaviour and protective quality of sputtered chromium nitride coatings, Surf. Coatings Technol 126 (2000) 199–209, https://doi.org/10.1016/S0257-8972(00)00527-2.

[27] H.M. Abd El-Lateef, I.M.A. Mohamed, J.H. Zhu, M.M. Khalaf, An efficient synthesis of electrospun TiO2-nanofibers/Schiff base phenylalanine composite and its inhibition behavior for C-steel corrosion in acidic chloride environments, J. Taiwan Inst. Chem. Eng. 112 (2020) 306–321, https://doi.org/10.1016/j.jtice.2020.06.002.

[28] H.R. Bakhsheshi-Rad, M. Akbari, A.F. Ismail, M. Aziz, Z. Hadisi, E. Pagan, M. Daroonparvar, X. Chen, Coating biodegradable magnesium alloys with electrospun poly-L-lactic acid-åkermanite-doxycycline nanofibers for enhanced biocompatibility, antibacterial activity, and corrosion resistance, Surf. Coatings Technol 377 (2019), 124898, https://doi.org/10.1016/j.surfcoat.2019.124898.

[29] Z. Panahi, E. Tamjid, M. Rezaei, Surface modification of biodegradable AZ91 magnesium alloy by electrospun polymer nanocomposite: Evaluation of in vitro degradation and cytocompatibility, Surf. Coatings Technol 386 (2020), 125461, https://doi.org/10.1016/j.surfcoat.2020.125461.

[30] M. Karimi Kichi, R. Torkaman, H. Mohammadi, A. Toutounchi, M. Kharaziha, F. Alihosseini, Electrochemical and in vitro bioactivity behavior of poly (ε-caprolactone) (PCL)-gelatin-forsterite nano coating on titanium for biomedical application, Mater. Today Commun (2020) 24, https://doi.org/10.1016/j.mtcomm.2020.101326.

[31] D. Li, Y. Xia, Electrospinning of nanofibers: Reinventing the wheel? Adv. Mater 16 (2004) 1151–1170, https://doi.org/10.1002/adma.200400719.

[32] X. Zhao, S. Yuan, Z. Jin, Q. Zhu, M. Zheng, Q. Jiang, H. Song, J. Duan, Fabrication of composite coatings with core-shell nanofibers and their mechanical properties, anticorrosive performance, and mechanism in seawater, Prog. Org. Coatings 149 (2020), 105893, https://doi.org/10.1016/j.porgcoat.2020.105893.

[33] T. Hanas, T.S. Sampath Kumar, Tailoring Biodegradation of Fine Grained AZ31 Alloy Implants by Nanofibrous Coatings, Mater. Today Proc 4 (2017) 6697–6703, https://doi.org/10.1016/j.matpr.2017.06.444.

[34] Y. Yu, Y. Zuo, Z. Zhang, L. Wu, C. Ning, C. Zuo, Al2O3 coatings on zinc for anti-corrosion in alkaline solution by electrospinning, Coatings (2019) 9, https://doi.org/10.3390/coatings9110692.

[35] Y. Zhao, Z. Zhang, L. Yu, Q. Tang, Electrospinning of polyaniline microfibers for anticorrosion coatings: An avenue of enhancing anticorrosion behaviors, Synth. Met 212 (2016) 84–90, https://doi.org/10.1016/j.synthmet.2015.12.007.

[36] Y. Zhao, Z. Zhang, L. Yu, Corrosion protection of carbon steel by electrospun fi lm containing polyaniline micro fi bers, 102 (2016) 20–26. 10.1016/j.reactfunctpolym.2016.03.007.

[37] P.J. Rivero, D.M. Redin, R.J. Rodríguez, Electrospinning: A powerful tool to improve the corrosion resistance of metallic surfaces using nanofibrous coatings, Metals (Basel) (2020) 10, https://doi.org/10.3390/met10030350.

[38] J. Kim, H.M. Mousa, C. Hee, C. Sang, Applied Surface Science Enhanced corrosion resistance and biocompatibility of AZ31 Mg alloy using PCL / ZnO NPs via electrospinning, Appl. Surf. Sci 396 (2017) 249–258, https://doi.org/10.1016/j.apsusc.2016.10.092.

[39] R. Augustine, N. Kalarikkal, S. Thomas, Effect of zinc oxide nanoparticles on the in vitro degradation of electrospun polycaprolactone membranes in simulated body fluid, Int. J. Polym. Mater. Polym. Biomater 65 (2016) 28–37, https://doi.org/10.1080/00914037.2015.1055628.

[40] M. Karthega, M. Pranesh, C. Poongothai, N. Srinivasan, Poly caprolactone/titanium dioxide nanofiber coating on AM50 alloy for biomedical application, J. Magnes. Alloy (2020), https://doi.org/10.1016/j.jma.2020.07.003.

[41] H.R. Bakhsheshi-Rad, A.F. Ismail, M. Aziz, Z. Hadisi, M. Omidi, X. Chen, Antibacterial activity and corrosion resistance of Ta 2 O 5 thin film and electrospun PCL/MgO-Ag nanofiber coatings on biodegradable Mg alloy implants, Ceram. Int 45 (2019) 11883–11892, https://doi.org/10.1016/j.ceramint.2019.03.071.

[42] X. Yang, C. Shao, H. Guan, X. Li, J. Gong, Preparation and characterization of ZnO nanofibers by using electrospun PVA/zinc acetate composite fiber as precursor, Inorg. Chem. Commun 7 (2004) 176–178, https://doi.org/10.1016/j.inoche.2003.10.035.

[43] H. Guan, C. Shao, S. Wen, B. Chen, J. Gong, X. Yang, Preparation and characterization of NiO nanofibres via an electrospinning technique, Inorg. Chem. Commun 6 (2003) 1302–1303, https://doi.org/10.1016/j.inoche.2003.08.003.

[44] H. Rodríguez-Tobías, G. Morales, A. Ledezma, J. Romero, R. Saldívar, V. Langlois, E. Renard, D. Grande, Electrospinning and electrospraying techniques for designing novel antibacterial poly(3-hydroxybutyrate)/zinc oxide nanofibrous composites, J. Mater. Sci. 51 (2016) 8593–8609, https://doi.org/10.1007/s10853-016-0119-x.

[45] R. Augustine, H.N. Malik, D.K. Singhal, A. Mukherjee, D. Malakar, N. Kalarikkal, S. Thomas, Electrospun polycaprolactone/ZnO nanocomposite membranes as biomaterials with antibacterial and cell adhesion properties, J. Polym. Res (2014) 21, https://doi.org/10.1007/s10965-013-0347-6.

[46] L.D. Tijing, Y.C. Woo, W.G. Shim, T. He, J.S. Choi, S.H. Kim, H.K. Shon, Superhydrophobic nanofiber membrane containing carbon nanotubes for high-performance direct contact membrane distillation, J. Memb. Sci. 502 (2016) 158–170, https://doi.org/10.1016/j.memsci.2015.12.014.

[47] A. Yakubu, Z. Abbas, N.A. Ibrahim, A. Fahad, Reduction of electromagnetic interference using zno-pcl nanocomposites at microwave frequency, Adv. Mater. Sci. Eng. 2015 (2015), https://doi.org/10.1155/2015/132509.

[48] J. Kim, H.M. Mousa, C.H. Park, C.S. Kim, Enhanced corrosion resistance and biocompatibility of AZ31 Mg alloy using PCL/ZnO NPs via electrospinning, Appl. Surf. Sci 396 (2017) 249–258, https://doi.org/10.1016/j.apsusc.2016.10.092.

[49] S. John, A. Joseph, A.J. Jose, B. Narayana, Enhancement of corrosion protection of mild steel by chitosan/ZnO nanoparticle composite membranes, Prog. Org. Coatings 84 (2015) 28–34, https://doi.org/10.1016/j.porgcoat.2015.02.005.

[50] H. Guan, C. Shao, B. Chen, J. Gong, X. Yang, A novel method for making CuO superfine fibres via an electrospinning technique, Inorg. Chem. Commun 6 (2003) 1409–1411, https://doi.org/10.1016/j.inoche.2003.08.021.

[51] C. Shao, X. Yang, H. Guan, Y. Liu, J. Gong, Electrospun nanofibers of NiO/ZnO composite, Inorg. Chem. Commun 7 (2004) 625–627, https://doi.org/10.1016/j.inoche.2004.03.006.

[52] D. Mareci, A. Cailean, G. Ciurescu, D. Sutiman, Electrochemical Determination of the Corrosion Resistance of NiCr Dental Casting Alloys~!2009-10-19~!2010-03-31~!2010-06-02~!, Open Corros. J 3 (2010) 45–53, https://doi.org/10.2174/1876503301003010045.

[53] B. Yao, G. Wang, J. Ye, X. Li, Corrosion inhibition of carbon steel by polyaniline nanofibers, Mater. Lett 62 (2008) 1775–1778, https://doi.org/10.1016/j.matlet.2007.10.001.

[54] B Wessling, Passivation of Metals by Coating with Polyaniline: Corrosion Potential Shift and Morphological Changes, Adv. Mater 6 (1994) 226–228, 10.1002/)).

[55] N. Ahmad, A.G. MacDiarmid, Inhibition of corrosion of steels with the exploitation of conducting polymers, Synth. Met 78 (1996) 103–110, https://doi.org/10.1016/0379-6779(96)80109-3.

[56] Y. Zhao, Z. Zhang, L. Yu, T. Jiang, Hydrophobic polystyrene/electro-spun polyaniline coatings for corrosion protection, Synth. Met 234 (2017) 166–174, https://doi.org/10.1016/j.synthmet.2017.11.005.

[57] P.C. Okafor, X. Liu, Y.G. Zheng, Corrosion inhibition of mild steel by ethylamino imidazoline derivative in CO2-saturated solution, Corros. Sci 51 (2009) 761–768, https://doi.org/10.1016/j.corsci.2009.01.017.

[58] R. Arrabal, J.M. Mota, A. Criado, A. Pardo, M. Mohedano, E. Matykina, Assessment of duplex coating combining plasma electrolytic oxidation and polymer layer on AZ31 magnesium alloy, Surf. Coatings Technol 206 (2012) 4692–4703, https://doi.org/10.1016/j.surfcoat.2012.05.091.

[59] X. Ji, W. Wang, W. Li, X. Zhao, A. Liu, X. Wang, X. Zhang, W. Fan, Y. Wang, Z. Lu, S. Liu, H. Shi, pH-responsible self-healing performance of coating with dual-action core-shell electrospun fibers, J. Taiwan Inst. Chem. Eng. 104 (2019) 227–239, https://doi.org/10.1016/j.jtice.2019.06.022.

[60] R. Solmaz, G. Kardaş, M. Çulha, B. Yazici, M. Erbil, Investigation of adsorption and inhibitive effect of 2-mercaptothiazoline on corrosion of mild steel in hydrochloric acid media, Electrochim. Acta 53 (2008) 5941–5952, https://doi.org/10.1016/j.electacta.2008.03.055.

[61] M. Özcan, I. Dehri, M. Erbil, Organic sulphur-containing compounds as corrosion inhibitors for mild steel in acidic media: Correlation between inhibition efficiency and chemical structure, Appl. Surf. Sci 236 (2004) 155–164, https://doi.org/10.1016/j.apsusc.2004.04.017.

[62] R. Solmaz, Investigation of the inhibition effect of 5- ((E) -4-phenylbuta-1, 3-dienylideneamino) - 1, 3, 4-thiadiazole-2-thiol Schiff base on mild steel corrosion in hydrochloric acid, Corros. Sci 52 (2010) 3321–3330, https://doi.org/10.1016/j.corsci.2010.06.001.

[63] Ž.Z. Tasić, M.B.Petrović Mihajlović, M.B. Radovanović, A.T. Simonović, M. M. Antonijević, Cephradine as corrosion inhibitor for copper in 0.9% NaCl solution, J. Mol. Struct. 1159 (2018) 46–54, https://doi.org/10.1016/j.molstruc.2018.01.031.

[64] C. Xing, Z. Zhang, L. Yu, L. Zhang, G.A. Bowmaker, Electrochemical corrosion behavior of carbon steel coated by polyaniline copolymers micro/nanostructures, RSC Adv. 4 (2014) 32718–32725, https://doi.org/10.1039/c4ra05826g.